Supporting Information

Bioinspired molecular catalysts with unique tricopper architecture for highly efficient oxygen reduction reaction

Peng-Peng Guo, Chao Xu, Kun-Zu Yang, Chen Lu, Hua-Min Chi, Ying Xu, Yong-Zhi Su, Xin Liu, Ping-Jie Wei and Jin-Gang Liu*

Key Laboratory for Advanced Materials, School of Chemistry & Molecular Engineering, East China University of Science and Technology, Shanghai 200237, P. R. China

E-mail: liujingang@ecust.edu.cn

1. Materials and Characterizations.

All reagents and solvents utilized in this paper were of analytical grade, which were obtained from commercial suppliers and were used directly without further purification. Aqueous solutions were prepared from high purity water (⩾18.25 MΩ·cm). Powder X-ray diffraction (PXRD) measurements were performed on an X-ray powder diffractometer (D/max2550 V, Rigaku Japan) in the range 5-50° at room temperature. Materials' morphologies were recorded on Transmission electron microscopy (TEM; JEM-1400). X-ray absorption fine structure was recorded at the 1W1B station of the BSRF. The metal contents of the samples were examined by ICP-AES (Perkin Elmer Ltd., USA).

2. Experiment Section

2.1 Synthesis of carboxymethyl cellulose-derived carbon (CMC)

Carboxymethyl cellulose-derived carbon (CMC) was prepared through a two-step process involving the formation of a precursor gel and subsequent carbonization. Initially, 2.0 g of carboxymethyl cellulose and 2.0 g of urea were combined in a beaker and vigorously stirred with 30 mL of distilled water until a homogeneous gel-like mixture was formed. The gel was then subjected to a freeze-drying process to remove the solvent and obtain a white solid sample. Subsequently, the freeze-dried sample was placed in a nitrogen-filled tube furnace and gradually heated to 900 °C at a rate of 5 °C per minute. The temperature was maintained at 900 °C for 1 hour

to allow for complete carbonization. After natural cooling of the furnace, the carbonized sample was retrieved, resulting in the production of carboxymethyl cellulose-derived carbon (CMC).

2.2 Synthesis of CMC-nCu$_3$

Initially, 0.5 mmol (121 mg) of copper nitrate trihydrate, 0.5 mmol (96 mg) of 3,3',5,5'-tetramethyl-4,4'-bipyrazole, and 100 mg of CMC were combined in a 5 mL mixture of 1:1 (v/v) ammonia (25-28%) and methanol. The mixture was sonicated for 5 minutes to ensure thorough dispersion of the components, followed by stirring at room temperature for 15 minutes. The reaction mixture was then transferred to a reaction vessel and heated to 180 ℃ for 48 hours under continuous stirring. Afterwards the mixture was allowed to cool to room temperature. The resulting precipitate was collected by centrifugation and washed several times with methanol to remove any unreacted species. The precipitate was then dried in an oven to obtain the desired CMC-nCu$_3$ product CMC-nCu$_3$-100. In order to optimize the performance of CMC-nCu$_3$, two additional molecular catalysts, CMC-nCu$_3$-50 and CMC-nCu$_3$-150, were synthesized by modifying the synthesis procedure to incorporate different amounts of CMC. 50 mg and 150 mg of CMC was used for the preparation of CMC-nCu$_3$-50 and CMC-nCu$_3$-150, respectively.

2.3 Synthesis of CN-Cuphen

Initially, 0.5 mmol (121 mg) of copper nitrate trihydrate, 1 mmol (198 mg) of 1,10-phenanthroline monohydrate, and 100 mg of CMC were combined in a 20 mL mixture of water and methanol (1:1 v/v). The reaction mixture was stirred at 60 ℃ for 10 hours. After the reaction completion, the solvent was evaporated under reduced pressure to obtain the solid CMC-CuPhen product.

3. Electrochemical Measurement

A catalyst (3.0 mg) was dispersed in a 150 μL mixture solution containing 5 wt% Nafion dispersion (Aldrich) and isopropanol with a volume ratio of 1:9 in a centrifuge tube. The mixture was sonicated for 20 minutes to achieve a uniform suspension, referred to as the catalyst ink. Subsequently, 5 μL of the catalyst ink was pipetted onto the surface of a glassy carbon disk with an area of 0.196 cm².The catalyst ink was allowed to dry naturally, resulting in an even film with a catalyst mass loading of 0.5 mg cm^{-2}. For comparison, the reference Pt/C catalyst was loaded with 0.3 mg cm^{-2}.

The electrochemical performance of the catalysts was evaluated using a CHI 760D

electrochemical workstation in a standard three-electrode system. A rotating ring-disk electrode (RRDE, Pine Instrument) served as the working electrode. A graphite rod (diameter: 4.0 mm) and a Hg/HgO electrode were employed as the counter and reference electrodes, respectively. Cyclic voltammetry (CV) and linear sweep voltammetry (LSV) were performed in an O_2-saturated 0.1 M KOH solution at a scan rate of 10 mV/s and room temperature. For the catalyst durability test, the chronoamperometric response of the catalysts was assessed at 0.55 V (vs. RHE) in O_2-saturated 0.1 M KOH solution while maintaining a rotation speed of 900 rpm.

For RRDE measurement: The H_2O_2 yield and electron transfer number (n) were calculated from the RRDE data using the following equation (**1**) and equation (**2**)

$$H_2O_2\,\% = \frac{200 \times I_r}{I_r + N \times I_d} \quad (\mathbf{1})$$

$$n = \frac{4 \times N \times I_d}{I_r + N \times I_d} \quad (\mathbf{2})$$

where I_d is the disk current, I_r is the ring current, and N is the collection efficiency.

RHE calibration: The calibration of the reference electrode was conducted in a H_2-saturated electrolyte with Pt wire as the working electrode. The potential at which the current crossed zero was regarded as the thermodynamic potential for the hydrogen electrode reactions.

4. Zinc-air batteries (ZABs)

Zn-air batteries (ZABs) were assembled using polished Zn foil as the anode, catalyst-loaded carbon paper (1.0 mg cm^{-2} catalyst loading) as the cathode, and an aqueous electrolyte containing 0.2 M $ZnAc_2$ and 6.0 M KOH. A reference sample employing commercial 20 wt.% Pt/C catalyst was prepared with the same loading amount (1.0 mg cm^{-2}) for comparison. The electrochemical performance of the assembled batteries was evaluated using a CHI 760D electrochemical workstation at room temperature.

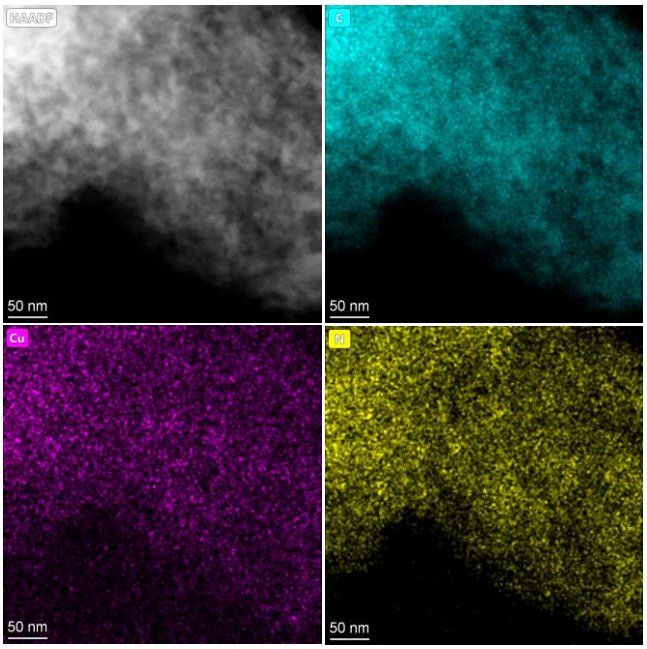

Figure S1. HAADF-STEM and the corresponding elemental mapping images of CMC-nCu_3, showing the distribution of C (cyan), Cu (purple), and N (yellow) elements.

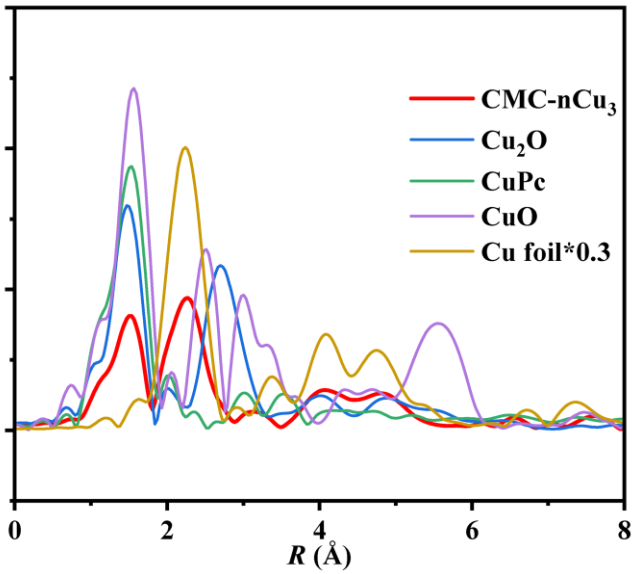

Figure S2. EXAFS spectra of CMC-nCu_3 and other reference samples as noted.

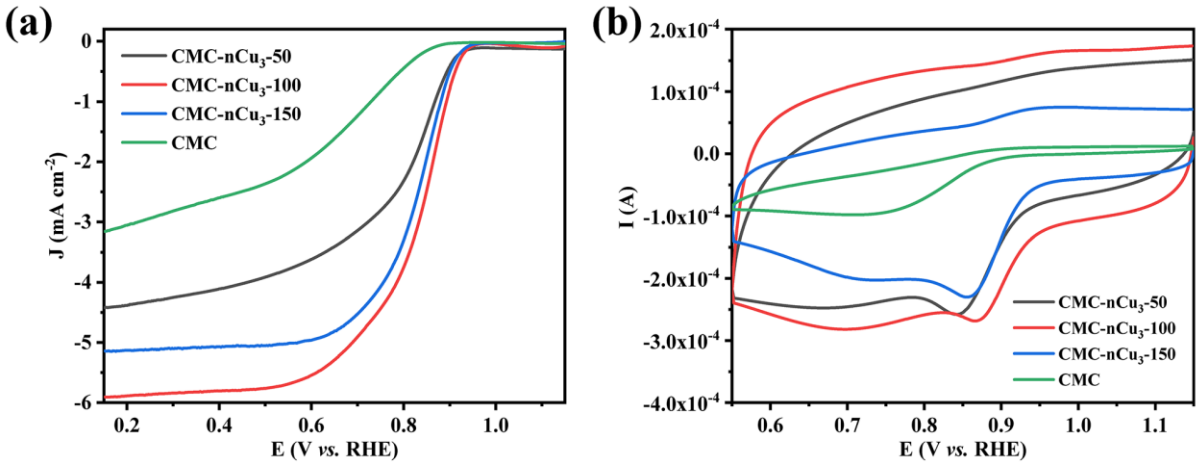

Figure S3. (a) LSV curves of CMC, CMC-nCu$_3$-x (x = 50, 100, 150) in O_2-saturated alkaline solution (0.1 M KOH) at 1600 rpm. **(b)** The CV curves of the catalysts.

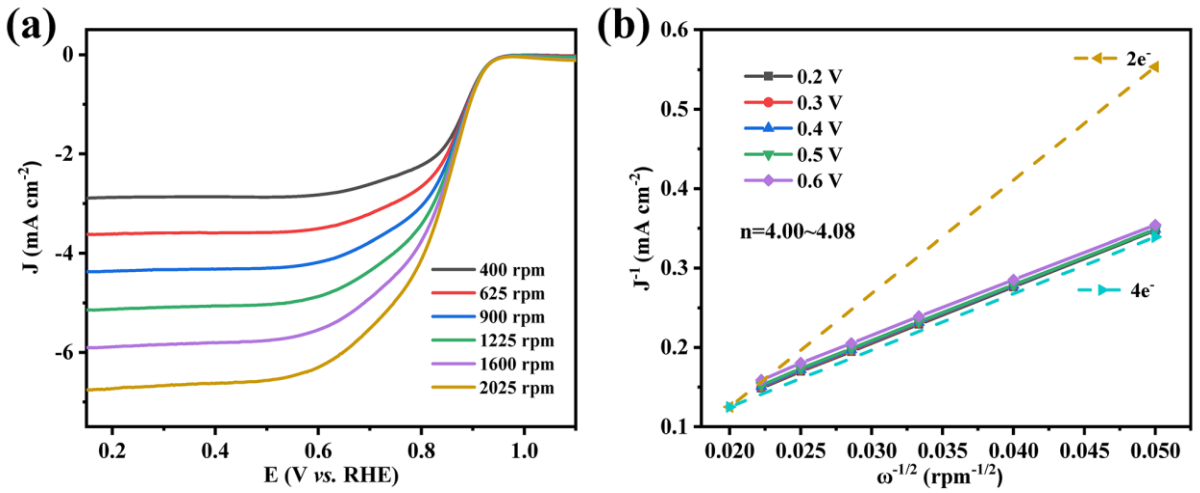

Figure S4. (a) LSV curves of CMC-nCu$_3$ in O_2-saturated 0.1 M KOH solution at different rotation rates (400-2025 rpm). **(b)** K-L plots for CMC-nCu$_3$ at 0.2 – 0.6 V.

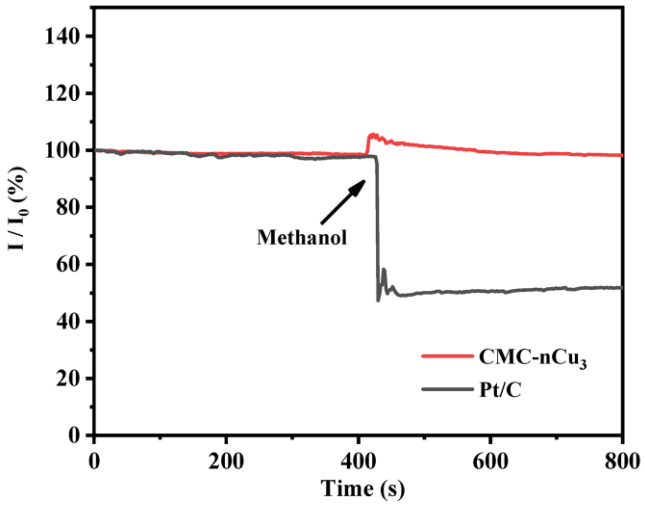

Figure S5. Methanol tolerance tests of CMC-nCu_3 and Pt/C.

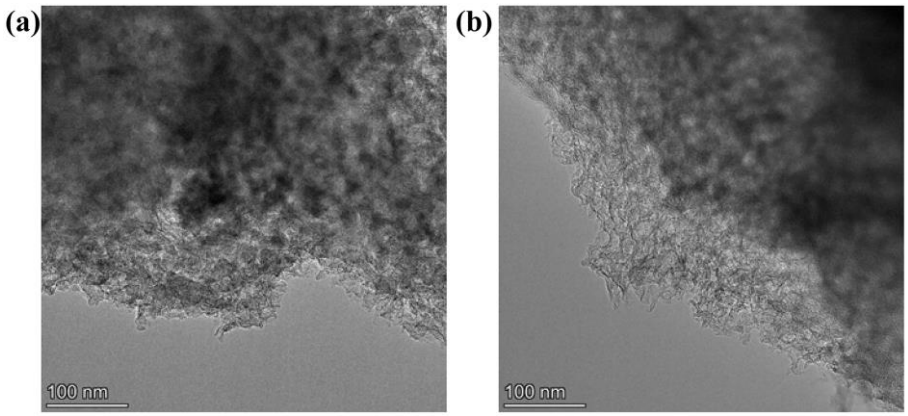

Figure S6. HR TEM images of CMC-nCu_3 before (a) and after (b) ADT evaluation.

Table S1. Performance of reported Cu-based molecular catalysts for ORR in alkaline solution.

Catalysts	$E_{1/2}$ (V vs. RHE)	Solution	Ref.
CMC-nCu_3	0.87	0.1 M KOH	This work
1-Cu	0.78	0.1 M KOH	1
Cu-COP	0.62	0.1 M KOH	2
Cu-POP	0.75	0.1 M KOH	3
PcCu-O_8-Co/CNTs	0.83	0.1 M KOH	4
Cu-1D-CP/C	~ 0.78	0.1 M KOH	5
Cu_3(7-N-Etppz(CH_2OH))	~ 0.74	0.1 M NaOH	6
Cu-BTC@AC	0.74	0.1 M KOH	7
MWCNTs@BTAHCu(II)	~ 0.71	0.1 M KOH	8
PVI-Cu($phen^{NO2}$)-PVI@CNTs	0.859	0.1 M KOH	9
polyCuDAB-CB	0.760	0.1 M KOH	10
Cu($tpfcBr_8$)	0.71	0.1 M KOH	11
CNTs@TiO_2-ZA-[Cu($phen^{NO2}$)(BTC)]	0.805	0.1 M KOH	12
Cu–CTF/CP	0.77	0.1 M NaOH	13
rGO-TADPyCu	0.795	0.1 M KOH	14

References:

[1] J. Meng, H. Qin, H. Lei, X. Li, J. Fan, W. Zhang, U.-P. Apfel and R. Cao, *Angew. Chem. Int. Ed.*, 2023, **62**, e202312255.

[2] Y.-F. Yao, Z.-Y. Huang, W.-Y. Xie, S.-J. Huang, Z.-Y. Liu, G. Yang, J.-S. Ye, H.-Y. Liu and X.-Y. Xiao, *Catal. Sci. Technol.*, 2023, **13**, 6321-6330.

[3] H. Lei, Q. Zhang, Z. Liang, H. Guo, Y. Wang, H. Lv, X. Li, W. Zhang, U.-P. Apfel and R. Cao, *Angew. Chem. Int. Ed.*, 2022, **61**, e202201104.

[4] H. Zhong, K. H. Ly, M. Wang, Y. Krupskaya, X. Han, J. Zhang, J. Zhang, V. Kataev, B. Büchner, I. M. Weidinger, S. Kaskel, P. Liu, M. Chen, R. Dong and X. Feng, *Angew. Chem. Int. Ed.*, 2019, **58**, 10677 -10682

[5] Y. P. Kharwar, S. Mandal and K. Ramanujam, *J. Electrochem. Soc.*, 2019, **166**, F3193-F3201.

[6] N. Thiyagarajan, D. Janmanchi, Y.-F. Tsai, W. H. Wanna, R. Ramu, S. I. Chan, J.-M. Zen and S. S. F. Yu, *Angew. Chem. Int. Ed.*, 2018, **57**, 3612-3616.

[7] S. Gonen, O. Lori, G. Cohen-Taguri and L. Elbaz, *Nanoscale*, 2018, **10**, 9634-9641.

[8] T. Gurusamy, P. Gayathri, S. Mandal and K. Ramanujam, *ChemElectroChem*, 2018, **5**, 1837-1847.

[9] F.-F. Wang, Y.-M. Zhao, P.-J. Wei, Q.-L. Zhang and J.-G. Liu, *Chem. Commun.*, 2017, **53**, 1514-1517.

[10] F. He, L. Mi, Y. Shen, X. Chen, Y. Yang, H. Mei, S. Liu, T. Mori and Y. Zhang, *J. Mater. Chem. A*, 2017, **5**, 17413-17420.

[11] N. Levy, A. Mahammed, A. Friedman, B. Gavriel, Z. Gross and L. Elbaz, *ChemCatChem*, 2016, **8**, 2832-2837.

[12] F.-F. Wang, P.-J. Wei, G.-Q. Yu and J.-G. Liu, *Chem. Eur. J.*, 2016, **22**, 382-389.

[13] K. Iwase, T. Yoshioka, S. Nakanishi, K. Hashimoto and K. Kamiya, *Angew. Chem. Int. Ed.*, 2015, **54**, 11068-11072.

[14] Y.-T. Xi, P.-J. Wei, R.-C. Wang and J.-G. Liu, *Chem. Commun.*, 2015, **51**, 7455-7458.